Published in final edited form as:
Free Radic Biol Med. 2009 January 15; 46(2): 220–231. doi:10.1016/j.freeradbiomed.2008.10.025.

The Cinnamon-derived Michael Acceptor Cinnamic Aldehyde Impairs Melanoma Cell Proliferation, Invasiveness, and Tumor Growth

Christopher M. Cabello, **Warner B. Bair 3rd**, **Sarah D. Lamore**, **Stephanie Ley**, **Alexandra S. Bause**, **Sara Azimian**, and **Georg T. Wondrak***
Department of Pharmacology and Toxicology, College of Pharmacy, Arizona Cancer Center, University of Arizona, Tucson, AZ, USA

Abstract

Redox dysregulation in cancer cells represents a chemical vulnerability that can be targeted by prooxidant redox intervention. Dietary constituents that contain an electrophilic Michael acceptor pharmacophore may therefore display promising chemopreventive and chemotherapeutic anti-cancer activity. Here, we demonstrate that the cinnamon-derived dietary Michael acceptor trans-cinnamic aldehyde (CA) impairs melanoma cell proliferation and tumor growth. Feasibility of therapeutic intervention using high doses of CA (120 mg/kg, p.o., q.d., 10 days) was demonstrated in a human A375 melanoma SCID-mouse xenograft model. Low micromolar concentrations (IC_{50} < 10 μM) of CA, but not closely related CA-derivatives devoid of Michael acceptor activity, suppressed proliferation of human metastatic melanoma cell lines (A375, G361, LOX) with G1 cell cycle arrest, elevated intracellular ROS, and impaired invasiveness. Expression array analysis revealed that CA induced an oxidative stress response in A375 cells, up-regulating heme oxygenase-1 (HMOX1), sulfiredoxin 1 homolog (SRXN1), thioredoxin reductase 1 (TXNRD1), and other genes including the cell cycle regulator and stress-responsive tumor suppressor gene cyclin-dependent kinase inhibitor 1A (CDKN1A), a key mediator of G1 phase arrest. CA, but not Michael-inactive derivatives, inhibited NFκB transcriptional activity and TNFα-induced IL-8 production in A375 cells. These findings support a previously unrecognized role of CA as a dietary Michael acceptor with potential anticancer activity.

Keywords

melanoma; oxidative stress; Michael acceptor; cinnamic aldehyde; NFκB; p21 (CDKN1A); xenograft

Introduction

Melanoma is a highly invasive and metastatic tumor that affects fair-skinned Caucasian populations worldwide with an annual increase in incidence rate between 3–7% [1]. In the United States, the incidence of malignant melanoma has increased steadily, where the lifetime

*Address correspondence to: Georg T. Wondrak, Ph.D. University of Arizona, Arizona Cancer Center, 1515 North Campbell Avenue, Tucson, AZ 85724 USA, E-mail: wondrak@pharmacy.arizona.edu, Telephone: 520-626-9017, FAX: 520-626-8567.

risk of developing melanoma was 1 in 68 individuals in the year 2002 [1]. Metastatic melanoma displays a notorious resistance to conventional chemotherapy, and the persistent dearth of effective treatment modalities creates an urgent need for novel pharmacological agents for melanoma chemoprevention and chemotherapy [2–5].

Recent research suggests that in melanoma, redox dysregulation contributes to malignant transformation and progression that involves reactive oxygen species (ROS)-mediated mitogenic signaling and modulation of apoptotic and survival pathways including nuclear factor κB (NFκB) and Akt [6–9]. For example, constitutive activation of NFκB signaling in human melanoma cells from autocrine generation of ROS contributes to proliferative signaling and resistance to chemotherapeutic induction of apoptosis and can be antagonized by antioxidant intervention [6,10]. Indeed, accumulative evidence supports the hypothesis that altered redox signaling and regulation in melanoma and other cancer cells represent a chemical vulnerability that can be targeted by small molecule redox modulators including anti- and prooxidants [8,9,11,12]. Selective prooxidant redox intervention using small molecule electrophiles that substantially increase cellular ROS and thereby induce deviations from redox homeostasis that cannot be tolerated by malignant cells already under high constitutive oxidative stress has shown promise in cell culture-based systems [13,14], animal xenograft models [15,16], and clinical trials [12,17,18].

Based on the emerging role of pro-oxidant therapeutics in anti-cancer intervention we hypothesized that dietary constituents containing an electrophilic Michael acceptor pharmacophore may display promising chemopreventive and chemotherapeutic activity. Prototype Michael acceptors of the α,β-unsaturated aldehyde-class including acrolein, crotonaldehyde, and trans-4-hydroxy-2-nonenal display very high electrophilicity and chemical reactivity that are associated with cytotoxicity, carcinogenic potential, and an acute toxicity profile unacceptable for controlled systemic delivery and therapeutic testing *in vivo* [19–22]. In our search for a drug-like Michael acceptor with potential anticancer activity and established animal pharmacokinetics devoid of dose-limiting systemic toxicity we have focused our studies on trans-cinnamic aldehyde (cinnamaldeyde, trans-3-phenylpropenal, CA), the key flavor compound in cinnamon essential oil extracted from Cinnamomum zeylanicum and Cinnamomum cassia bark, an important dietary factor and food additive that contains an α,β-unsaturated carbonyl Michael pharmacophore [23,24]. Remarkably, CA is the only α,β-unsaturated aldehyde which is FDA-approved for use in foods (21 CFR § 182.60) and given the ‘Generally Recognized As Safe’ status by the ‘Flavor and Extract Manufacturers’ Association (FEMA) in the United States (FEMA no. 2286, 2201) [25]. Indeed, recent research in endothelial cell culture has examined the differential cytotoxicity associated with CA versus acrolein, the minimal Michael acceptor pharmacophore contained in CA [26]. The more reactive electrophile acrolein displayed strongly enhanced cytotoxicity in direct comparison to the less reactive Michael acceptor CA confirming the very low cytotoxicity of this dietary factor. Antioxidant [27], antimicrobial [28], anti-pyretic [29], anti-inflammatory [30], and anti-diabetic [31] activities of cinnamon have been attributed to cellular effects of CA and other cinnamon ingredients including phenolic proanthocyanidins. Recently, we have demonstrated that CA spontaneously forms covalent adducts with model thiols and activates Nrf2-regulated antioxidant response element (ARE)-mediated gene expression in cultured human skin cells suggesting a photo-chemopreventive activity of this dietary Michael acceptor [32]. Here we demonstrate that (*I*) CA, but not closely related CA-derivatives devoid of Michael acceptor activity, impairs melanoma cell proliferation, viability, invasiveness, and NFκB transcriptional activity, and that (*II*) high oral doses of CA display significant anti-melanoma activity in an animal model of the disease.

Material and Methods

Chemicals

All chemicals were from Sigma Chemical Co, St. Louis, MO.

Human Melanoma SCID mouse xenograft model

A375 human melanoma cells were grown in HyQ RPMI-1640 media (HyClone) supplemented with 10% fetal bovine serum (Omega Scientific), and maintained in 5% CO_2-95% air humidified atmosphere at 37°C. Subconfluent cells were harvested by using 0.25% trypsin-EDTA (HyClone). Cells (>90% viability) were resuspended at the concentration of 10×10^6 cells/100μl of sterile saline. A SCID mouse colony was developed at the University of Arizona using original SCID (C.B-17/IcrACCSCID) obtained from Taconic (Germantown, New York). The mice were housed in microisolator cages (Allentown Caging Equipment Company, Allentown, N.J.) and maintained under specific pathogen-free conditions. Every month mice were screened by ELISA serology for mycoplasma, mouse hepatitis virus, pinworms, and Sendai virus and tested negative. SCID mice 6–8 weeks of age were bled (<200 μl) by retroorbital puncture in order to screen for the presence of mouse IgG using an ELISA. Only mice with IgG levels ≤ 20 ug/ml were used for the experiments. The mice ate NIH-31 irradiated pellets (Tekland Premier, Madison, WI) and received autoclaved water. Animal facilities are approved by the Association for the Assessment and Accreditation of Laboratory Animal Care International and in accordance with United States Department of Agriculture, Department of Health and Human Services, and NIH regulations. A375 cell injections (10×10^6 cells) were given subcutaneously on the mouse's lower right flank on day 0, and after tumors became established (~65 mm^3) mice were pair-matched into the treatment groups. The following day, treatment with CA or carrier only was initiated. The chemotherapeutic test agent CA was prepared and administered by oral gavage in less than 1 hour. CA (120 mg/kg/d in 0.5% methylcellulose/PBS, 100 μl p.o., n=10) was given on days 1–10 post the day of pair-matching, whereas control animals received carrier only (n=12). Subcutaneous tumors were measured twice weekly for tumor volume estimation (mm^3) in accordance with the formula $(a^2 \times b)/2$ where a is the smallest diameter and b is the largest diameter. The mice were sacrificed individually by CO_2 when the tumors reached a volume of 2000 mm^3. Tumor growth curves were obtained by determining average tumor volumes until day 30 after cell injection, and data points were analyzed using the two-sided Student's *t* test (*, $p < 0.05$; **, $p < 0.01$; ***, $p < 0.001$). All procedures were completed in accordance with the University of Arizona Institutional Animal Care and Use Committee (IACUC) protocol (# 07-029, approved May 24, 2007).

Immunohistochemical characterization of tumor tissue from mice xenografts

At the end of the experiment, tumors from SCID mice were harvested and tumor tissue sections were analyzed for expression of the proliferation marker PCNA. Briefly, tissues were harvested, fixed in 10% neutral buffered formalin for 24 hours, processed and embedded in paraffin. Routine hematoxylin stain was performed on three micron sections of tissue and immunohistochemistry was performed using a mouse monoclonal antibody to PCNA (clone PC10, Zymed (#18-0110), used at 1:1500). Detection of primary antibody was performed on a Discovery XT Automated Immunostainer (Ventana Medical Systems, Inc, Tucson, Arizona) using a biotinylated-streptavidin-HRP and DAB system. Hematoxylin counterstaining was also performed online. Following staining on the instrument, slides were dehydrated through graded alcohols to xylene and coverslipped with Pro-Texx mounting medium. Images were captured using an Olympus BX50 and Spot (Model 2.3.0) camera. Images were standardized for light intensity. No automated analysis of the data was performed.

General cell culture

G-361 Human melanoma cells from ATCC (Manassas, VA, USA) were cultured in McCoy's 5a medium containing 10% bovine calf serum (BCS). Human A375 and LOX metastatic melanoma cells (ATCC) were cultured in RPMI medium containing 10% BCS and 2 mM L-glutamine. Human HT29 and HCT116 colon carcinoma cells (ATCC) were cultured in RPMI containing 10% BCS. Dermal neonatal foreskin Hs27 fibroblasts from ATCC were cultured in DMEM containing 10% fetal bovine serum. Primary human epidermal keratinocytes (neonatal HEKn-APF, from Cascade Biologics, Portland, OR) were cultured using Epilife medium supplemented with EDGS growth supplement and passaged using recombinant trypsin/EDTA and defined trypsin inhibitor. Cells were maintained at 37 °C in 5% CO_2, 95% air in a humidified incubator.

Cell proliferation assay

Cells were seeded at 10,000 cells/dish on 35-mm dishes. After 24 h, cells were treated with a dose range of test compounds (CA and CA-derivatives DHCA, COH, and CAC). Cell numbers at the time of compound addition and 72 h later were determined using a Z2 Analyzer (Beckman Coulter, Inc., Fullerton, CA). Proliferation was compared with cells that received mock treatment. The same methodology was used to establish IC_{50} values (drug concentration that induces 50% inhibition of proliferation of treated cells within 72 h exposure ± SD, n = 3) of anti-proliferative potency against melanoma and colon cancer cell lines.

Cell cycle analysis using bivariate flow cytometric detection of BrdU incorporation and DNA content

Human A375 melanoma cells were exposed to CA (20 μM, 24 and 48 h), and bivariate cell cycle analysis was performed by flow cytometric determination of cellular DNA synthesis (BrdU incorporation) and DNA content (7-AAD staining) using the FITC-BrdU Flow Kit (BD Pharmingen, San Jose, CA) according to the manufacture's protocol. Briefly, cells were seeded at 1×10^6 cells per T-75 cell culture flask. After 24 h cells received treatment (CA, 20 μM or mock). After 48 h exposure, BrdU (20 μM, 45 min) pulse labeling of cells undergoing DNA synthesis was performed. Cells were harvested immediately after by trypsinization. After fixation and permeabilization, cells were treated with DNase (300 μg/ml in DPBS, 1 h, 37°C). Cells were then stained for BrdU-epitopes using a FITC-conjugated anti-BrdU antibody and for DNA content using 7-AAD, followed by bivariate flow cytometric analysis. Cell fractions in G1, S, and G2/M phase, respectively, were expressed in percent of total gated cells (mean ± SD, n=3).

Apoptosis analysis and assessment of cytotoxicity

Viability and induction of cell death (early and late apoptosis/necrosis) were examined by annexin-V-FITC/propidium iodide (PI) dual staining of cells followed by flow cytometric analysis as published previously [33,34]. Cells (100,000) were seeded on 35 mm dishes and received drug treatment 24 hours later. Cells were harvested at various time points after treatment and cell staining was performed using an apoptosis detection kit according to the manufacturer's specifications (APO-AF, Sigma, St. Louis, MO).

Caspase-3 activation assay

Treatment-induced caspase-3 activation was examined in A375 melanoma cells using a cleaved/activated caspase-3 (asp 175) antibody (Alexa Fluor 488 conjugate, Cell Signaling, Inc.) followed by flow cytometric analysis as published recently [14]. Briefly, cells were harvested at various time points after treatment, resuspended in PBS and fixed in 1% formaldehyde. Cells were then permabilized using 90% methanol and resuspended in incubation buffer (PBS, 0.5% BSA). After rinsing by centrifugation, cells were resuspended

in incubation buffer (90 μl) and cleaved caspase-3 antibody (10 μl) was added. After incubation (40 min) followed by rinsing and centrifugation in incubation buffer, cells were resuspended in PBS and analyzed by flow cytometry.

Cell invasion assay

Melanoma cell invasion was determined using the CytoSelect™ Cell Invasion Assay (Cell Biolabs, Inc., San Diego, CA) according to manufacturer's instructions. Briefly, A375 cells were pre-treated with CA (10 or 20μM, 24 h). Basement membranes of Boyden chambers were rehydrated with 300 μL serum free RPMI, and 2.5×10^6 cells were then seeded into the upper area of the chamber in serum free RPMI. Bottom wells were filled with RPMI supplemented with 10% FBS containing CA or no CA. After 48 h incubation (37°C, 5% CO_2), non-invasive cells were removed from the upper chamber and cell invasion was assessed by light microscopy after staining of invaded cells with crystal violet Cell Stain Solution (Cell Biolabs). For colorimetric quantification of invasion, inserts were then placed in extraction buffer (200 μl, 10 min), and absorbance at 560 nm was determined after transfer to a 96 well plate (100 μl per well) using a VersaMax microtiter plate reader (Molecular Devices, Sunnyvale, CA).

Detection of intracellular oxidative stress by flow cytometric analysis

Induction of intracellular oxidative stress by CA was analyzed by flow cytometry using 2′,7′-dichlorodihydrofluorescein diacetate (DCFH-DA) as a sensitive non-fluorescent precursor dye according to a published standard procedure [14,35]. Human A375 melanoma cells were treated with CA (10, 20, and 40 μM, 24 h) followed by DCFH-DA loading. To this end, cells were incubated for 60 min in the dark (37°C, 5% CO_2) with culture medium containing DCFH-DA (5 μg/mL final concentration). Cells were then harvested, washed with PBS, resuspended in 300 μl PBS and immediately analyzed by flow cytometry.

Determination of total cellular glutathione content

Pharmacological modulation of intracellular glutathione content was analyzed using the photometric HT Glutathione Assay Kit (Trevigen, Gaithersburg, MD) performed in 96 well format. This kinetic assay is based on the enzymatic recycling method involving glutathione reductase and DTNB (5,5′-dithiobis-2-nitrobenzoic acid, Ellman's reagent) to produce yellow colored 5-thio-2-nitrobenzoic acid (TNB) that absorbs at 405 nm. Human A375 melanoma (1×10^6) cells were exposed to a dose range of CA (10, 20, and 40 μM, 24 h) and harvested by trypsinization followed by sample processing according to the manufacturer's instructions. Oxidized glutathione was determined separately after 4-vinylpyridine-derivatization. Glutathione content of total cellular extracts was normalized to protein content determined using the BCA assay (Pierce, Rockford, IL).

RT^2 Human Oxidative Stress Profiler™ PCR Expression Array

After pharmacological exposure, total cellular RNA (3×10^6 A375 melanoma cells) was prepared according to a standard procedure using the RNeasy kit (Qiagen, Valencia, CA). Reverse transcription was performed using the RT^2 First Strand kit (SA Biosciences, Frederick, MD) and 5 μg total RNA. The RT^2 Human Oxidative Stress Profiler™ PCR Expression Array (SuperArray, Frederick, MD) profiling the expression of 84 oxidative stress-related genes was run using the following PCR conditions: 95 °C for 10 min, followed by 40 cycles of 95 °C for 15 sec alternating with 60 °C for 1 min (Applied Biosystems 7000 SDS). Gene-specific product was normalized to GAPDH and quantified using the comparative ($\Delta\Delta C_t$) Ct method as described in the ABI Prism 7000 sequence detection system user guide. Expression values were averaged across three independent array experiments, and standard deviation was calculated for graphing.

HMOX1, CDKN1A, SRXN1, TXNRD1, and GCLC expression analysis by real time RT-PCR

Total cellular RNA (3×10^6 cells) was prepared according to a standard procedure using the RNEasy kit from Qiagen. Reverse transcription was performed using TaqMan Reverse Transcription Reagents (Roche Molecular Systems, Branchburg, NJ) and 200 ng of total RNA in a 50 μl reaction. Reverse transcription was primed with random hexamers and incubated at 25 °C for 10 minutes followed by 48 °C for 30 minutes, 95°C for 5 minutes, and a chill at 4 ° C. Each PCR reaction consisted of 3.75 μl of cDNA added to 12.5 μl of TaqMan Universal PCR Master Mix (Roche Molecular Systems), 1.25 μl of gene-specific primer/probe mix (Assays-by-Design; Applied Biosystems, Foster City, CA) and 7.5 μl of PCR water. PCR conditions were: 95 °C for 10 minutes, followed by 40 cycles of 95 °C for 15 seconds, alternating with 60 °C for 1 minute using an Applied Biosystems 7000 SDS and Applied Biosystems' Assays On Demand primers specific to CDKN1A (p21, assay ID Hs00355782_m1), HMOX1 (heme oxygenase-1, assay ID Hs00157965_m1), SRXN1 (sulfiredoxin 1 homolog, assay ID Hs00607800_m1), TXNRD1 (thioredoxin reductase 1, assay ID Hs00182418_m1), and GCLC (glutamate-cysteine ligase, catalytic subunit, assay ID Hs00155249_m1). Gene-specific product was normalized to ACTB (β-actin, assay ID Hs99999903_m1; for GCLC) or glyceraldehyde-3-phosphate dehydrogenase (GAPDH, assay ID Hs99999905_m1; all other genes) and quantified using the comparative ($\Delta\Delta C_t$) Ct method as described in the ABI Prism 7000 sequence detection system user guide. Relative expression levels in response to mock treatment (control) and exposure to CA were determined in three repeat experiments (n=3, mean ± SD).

Heme oxygenase-1 immunoblot analysis

One day before treatment, 2×10^6 cells were seeded in T-75 flasks. Cell growth medium was replaced 24 h after seeding, followed by addition of test compounds 60 min after medium change. Cells were incubated for 24 h (37 °C, 5% CO_2), then washed with PBS, lysed in 1x SDS-PAGE sample buffer (200 μl, 0.375 M Tris HCl pH 6.8, 50% glycerol, 10% SDS, 5% β-mercaptoethanol, 0.25% bromophenol blue), and heated for 3 min at 95 °C. Separation by 15% SDS-PAGE and immunoblot analysis were performed as described earlier [32]. Equal protein loading was examined by actin-detection using a mouse anti-actin monoclonal antibody (Sigma, Saint Louis, MO).

p21 (Waf1/Cip1) immunoblot analysis

Cell extraction, SDS-PAGE, and Western transfer were performed as specified for heme oxygenase-1 immunoblot analysis. Mouse anti-p21 monoclonal antibody (Cell Signaling Technology, Boston, MA) was used 1:2000 in 5% milk-PBST overnight at 4° C. The membrane was washed three times for 10 min in 0.1% PBST before adding HRP-conjugated horse anti-mouse antibody (Cell Signaling Technology, Boston, MA) at 1:2000 dilution. Protein detection and loading control were performed as for heme oxygenase-1 immunoblotting.

NFκB Luciferase Reporter Assay

NFκB responsive TransLucent™ reporter vector, pNFκB-Luc, and empty TransLucent™ control reporter vector were purchased from Panomics (Fremont, CA). This vector contains multiple copies of the NFκB cis-acting enhancer element (*5′*GGGAATTTCCGGGAATT-TCCGGGAATTTCCGGGAATTTCCGGGAATTTCCGGAATTTCC3′) upstream of the Herpes simplex virus thymidine kinase TATA box promoter driving luciferase gene expression. A375 human melanoma cells were grown to 60% confluency in a 24 well plate. For transfection, 0.4 μg NFκB responsive TransLucent™ reporter vector, 0.8 ng promoterless Renilla reporter vector (phRG-B, Promega), 1.32μL Fugene6 (Roche), 20.68 μL OptiMEM I (Invitrogen) were added per well. Twenty-four hours after transfection, cells were treated with CA three hours prior to being stimulated with tumor necrosis factor alpha (TNFα) (20ng/mL;

Sigma) for 16 hours. Cells were then lysed in 100 μL passive lysis buffer using the Dual-Luciferase Reporter Assay System (Promega, Vienna, Austria) according to the manufacturer's instructions. Luciferase activity was measured with a Turner Designs TD20/20 luminometer. Data were reported as normalized averages of the Luciferase/Renilla ratio.

IL-8 Protein Expression

Human A375 melanoma cells were preincubated with or without CA (10 and 20 μM) for 3 h and stimulated with TNFα (20ng/mL, Sigma) or left untreated. Cellular IL-8 secretion was inhibited by addition of GolgiStop™ containing monensin (4 μl/6 ml cell culture medium, BD Biosciences, San Jose, CA) 15 min after TNFα addition. Intracytoplasmic IL-8 expression was examined 6 h later by flow cytometry using an Alexa-488 conjugated mouse monoclonal anti-human IL8 antibody (E8N1, Biolegend, San Diego, CA) according to the manufacturer's procedure.

Statistical Analysis

Unless indicated differently, the results are presented as means ± S.D. of at least three independent experiments. They were analyzed using the two-sided Student's *t* test (*, $p < 0.05$; **, $p < 0.01$; ***, $p < 0.001$).

Results

Oral administration of cinnamic aldehyde impairs growth of A375 human melanoma xenografts in SCID mice

Based on its known safety profile as human dietary factor, its documented low acute toxicity in mice (oral $LD_{50} > 2$ g/kg in mice [36]), and promising cell-based chemopreventive properties [32], we tested the thiol-reactive Michael acceptor CA as a potential inhibitor of tumor growth in a human melanoma SCID-mouse xenograft model (Fig. 1). Daily oral CA treatment (120 mg/kg/d in 0.5% methylcellulose/PBS) of human A375 melanoma xenograft bearing SCID mice induced a moderate suppression of tumor growth that reached the level of statistical significance ($p < 0.05$ versus carrier treated control) between days 18 to 30 after cell injection, where average tumor weights of CA-treated animals were up to 40% lower than that of carrier-treated controls (Fig. 1A). During CA treatment, no compound-related adverse reactions or average weight loss compared to carrier-treated control mice were observed suggesting the safety of administration of high doses of CA during the duration of the experiment (data not shown). Immunohistochemical staining of tumors revealed a pronounced downregulation of the cellular proliferation marker proliferating cell nuclear antigen (PCNA) in the nuclei of primary tumor tissue harvested from CA-treated versus carrier-treated mice (Fig. 1B), consistent with impairment of tumor cell proliferative capacity in xenograft-bearing mice treated with CA.

Taken together, these findings document for the first time feasibility of anti-melanoma intervention by oral administration of CA achieved at high doses in a mouse xenograft model.

Cinnamic aldehyde, but not its Michael-inactive chemical derivatives, suppresses proliferation of cultured human melanoma cells

After demonstrating chemotherapeutic efficacy of orally administered CA in a relevant animal model of the disease, molecular mechanisms of CA anti-melanoma activity were further examined in cell culture models. First, anti-proliferative activity of CA was assessed in cultured human A375 melanoma cells, where inhibition of cell proliferation was observed at low micromolar concentrations (Fig. 2 and Table 1). We then tested the structure-activity relationship of CA anti-proliferative activity using a colllection of closely related Michael-

active and Michael-inactive CA-derivatives as depicted in Fig. 2A [32]. In general, Michael-inactive CA-derivatives were found to be devoid of anti-proliferative activity over the dose range tested. Specifically, loss of αβ-unsaturation (as in dihydrocinnamic aldehyde, DHCA) or replacement of the carbonyl group by reduction (as in cinnamic alcohol, COH) or oxidation (cinnamic carboxylic acid, CAC) rendered CA inactive. In contrast, 4-methoxycinnamic aldehyde (MCA), a CA-derivative with intact Michael acceptor pharmacophore, maintained anti-proliferative activity against A375 melanoma cells (Fig. 2).

Next, anti-proliferative potency of CA was examined in a panel of three human melanoma [A375 (IC_{50}: 6.3 μM); G361 (IC_{50}: 8.1 μM); LOX (IC_{50}: 3.4 μM)] and two metastatic colon cancer [HT29 (IC_{50}: 19.7 μM); HCT116 (IC_{50}: 12.6 μM)] cell lines (Table 1). Anti-proliferative activity of CA against primary human skin keratinocytes [HEK (IC_{50}: 18.9 μM)] and fibroblasts [Hs27 (IC_{50}: 21.4 μM)] versus melanoma cell lines was observed at approximately two- to 6-fold higher concentrations suggesting that CA-associated anti-proliferative activity displays a moderate, yet significant degree of selectivity against human melanoma cell lines versus untransformed human skin cells. Bivariate flow cytometric cell cycle analysis measuring nuclear BrdU incorporation and DNA content confirmed anti-proliferative activity of CA against A375 cells (Fig. 3). Treatment with CA (20 μM) suppressed BrdU incorporation within 24 h of treatment (data not shown), and a pronounced G1-phase cell cycle arrest (2n cellular DNA content) with complete absence of cells in S-phase was observable after 48 h continuous exposure.

Based on these data, it was concluded that (*I*) CA exhibits potent anti-proliferative activity against human melanoma cell lines, (*II*) CA-inhibition of A375 melanoma cell proliferation does not occur with the Michael-inactive derivatives DHCA, COH, and CAC, and (*III*) CA-inhibition of melanoma cell proliferation occurs with suppression of DNA synthesis and cell cycle arrest in G1-phase.

Prolonged exposure to cinnamic aldehyde induces apoptosis with procaspase-3 cleavage in cultured human melanoma cells

Next, time course and dose-response of induction of A375 melanoma cell death by exposure to CA was assessed by flow cytometric analysis of annexinV-FITC/propidium iodide-stained cells (Fig. 4A). Only prolonged exposure (48 to 72 h) to CA at concentrations higher than 20 μM induced pronounced apoptosis. This finding was confirmed, when cleavage of procaspase-3, an independent marker of induction of apoptosis, was examined in A375 cells exposed to increasing doses of CA (10, 20, and 40 μM) for 3 d (Fig. 4B). Only at 40 μM CA, pronounced activation of caspase 3 was detected.

Cinnamic aldehyde suppresses human melanoma cell invasiveness

In an attempt to further explore the range of potential anti-melanoma activities of CA, suppression of melanoma cell invasiveness was assessed at sub-apoptogenic CA concentrations. To this end, melanoma cell invasion through basement membrane extracellular matrix of a Boyden chamber was examined using A375 cells left untreated or treated with CA (10 or 20 μM) (Fig. 5). Analysis by light microscopy (Fig. 5A) and colorimetry (Fig. 5B) revealed the potent anti-invasive effects of CA, with an approximately 75% reduction of cell invasion resulting from treatment with CA at 20 μM and a 30% reduction of cell invasion at 10 μM CA.

Cinnamic aldehyde induces a broad oxidative stress response in human A375 melanoma cells

After demonstrating anti-proliferative, apoptogenic, and anti-invasive activity of CA in simple melanoma cell culture models, induction of cellular oxidative stress and the modulation of

oxidative stress response gene expression was examined in A375 human melanoma cells exposed to CA at low micromolar concentrations. The RT^2 Human Oxidative Stress Profiler™ PCR Expression Array technology (SuperArray, Frederick, MD) was applied to A375 cells exposed to CA (25 μM, 24 h exposure) to assess expression of 84 stress-related genes contained on the array (Fig. 6A). CA-induced gene expression changes in A375 human melanoma cells affected 18 genes on the array by at least two-fold (Fig. 6A, right panel) including: oxidative stress response genes encoding the enzymes *heme oxygenase-1* (HMOX1; 129-fold), *glutathione peroxidase 2* (GPX2; 7-fold), *sulfiredoxin 1 homolog* (SRXN1; 7-fold), and *thioredoxin reductase 1* (TXNRD1; 4-fold); the oxidative stress-responsive transcription factors *early growth response gene 1* (EGR1; 5-fold) and *DNA-damage-inducible transcript 3* (DDIT3; 13-fold); and the redox-sensitive cell cycle regulator and stress-responsive tumor suppressor gene *cyclin-dependent kinase inhibitor 1A* (CDKN1A; 11-fold). Independent real time RT-PCR analysis then further confirmed upregulation of these genes as shown for HMOX1, SRXN1, TXNRD1, and CDKN1A (Fig. 6B). Next, CA-induced upregulation of cellular HMOX1 and CDKN1A gene expression was examined at the protein level by immunoblot analysis (Figs. 6C and 6D). Within 24 h, cellular heme oxygenase-1 protein levels were strongly upregulated upon exposure to CA (10 or 25 μM). Protein levels of p21, the CDKN1A gene product, were also strongly upregulated, but only in response to 25 μM CA.

Consistent with a mechanistic involvement of oxidative stress in the induction of a cellular response to CA treatment, a dose-dependent elevation of intracellular oxidative stress could be observed in A375 melanoma cells exposed to CA (10, 25, and 40 μM, 24 h) as assessed by 2′,7′-dichloro-dihydrofluorescein diacetate staining followed by flow cytometric analysis (Fig. 6E). In addition, modulation of cellular glutathione levels in A375 cells exposed to a dose range of CA was examined (Fig. 6F). Importantly, no glutathione depletion could be detected at low CA doses (10 and 20 μM) associated with the induction of cellular oxidative stress (Fig. 6E), inhibition of proliferation (Fig. 2A and table 1), and suppression of invasiveness (Fig. 5), strongly suggesting that anti-proliferative and anti-invasive effects of CA do not result from glutathione depletion. On the contrary, CA treatment (10 and 20 μM) increased cellular glutathione levels by up to 80%; in parallel, upregulation of GCLC (glutamate-cysteine ligase, catalytic subunit) gene expression, an important enzyme involved in glutathione biosynthesis not represented on the expression array, was observed (Fig. 6G) [37]. The ratio between reduced and oxidized glutathione did not change significantly at any CA concentration, and oxidized glutathione was always less than 3% of total glutathione (data not shown). These findings are consistent with earlier reports that document CA-induced Nrf2 activation and glutathione upregulation in other cell types [26,32]. However, moderate depletion of cellular GSH levels by approximately 15% was observed at higher, apoptogenic concentrations of CA (40 μM), suggesting that glutathione depletion may play a role in CA-induced cell death.

Taken together, these findings demonstrate that CA treatment at low micromolar concentrations induces specific redox alterations and upregulation of oxidative stress response gene expression in A375 melanoma cells.

Cinnamic aldehyde inhibits NFκB transcriptional activity and suppresses IL-8 in human melanoma cells

Recent research supports the causative role of altered redox signaling through NFκB in human melanoma [6,9,10]. The induction of redox alterations and oxidative stress response gene expression in CA-treated human melanoma cells as observed in Fig. 6, combined with an earlier report on CA-inhibition of NFκB signaling in human endothelial cells [38], lead us to examine the hypothesis that CA may inhibit signaling through this redox sensitive transcription factor in melanoma cells. To this end, A375 melanoma cells were co-transfected with a reporter plasmid containing the firefly luciferase gene under the control of the NFκB promoter and a

plasmid encoding renilla luciferase for normalization of transfection efficiency. First, pronounced suppression of constitutive NFκB transcriptional activity by almost 75% was observed in cells treated with CA (20 μM) for 12 h (Fig. 7A). Next, TNFα-induction (20ng/mL, 12h exposure) of NFκB transcriptional activity by approximately 15-fold was established in human melanoma cells (Fig. 7B). We then examined feasibility of suppression of TNFα-induced NFκB transcriptional activation by pretreating cells with CA, DHCA, COH, and CAC (20 μM each, 3h exposure) before TNFα treatment and determination of luciferase activity (Fig. 7B). Indeed, CA, but none of its Michael-inactive derivatives DHCA, COH, or CAC, suppressed TNFα-induced upregulation of luciferase activity by almost 85%, suggesting that CA treatment of melanoma cells may target signaling through NFκB. To gain further experimental support for an antagonistic effect of CA treatment on NFκB signaling in human melanoma cells, we examined the possibility that CA treatment inhibits TNFα-induced expression of IL-8, an inflammatory and invasion-promoting cytokine expressed in A375 melanoma cells in response to NFκB transcriptional activity (Fig. 8) [15,39]. To this end, A375 cells were pretreated with CA for 3 h and then stimulated by TNFα. After 6 h, IL-8 intracytoplasmic protein expression was then compared between CA (20 μM) and mock-pretreated cells by flow cytometric analysis (Fig. 8A). Indeed, CA pretreatment reduced TNFα-induced production of IL-8 to low levels characteristic of unstimulated cells. Inhibition of TNFα-induced IL-8 expression by CA occurred in the low micromolar range and followed a dose-response relationship with only partial suppression achieved by pretreatment with 10 μM and almost complete suppression observed after 20 μM CA (Fig. 8B).

Taken together these findings demonstrate that (I) CA inhibits constitutive and TNFα-induced NFκB transcriptional activity and (II) CA suppresses TNFα-induced upregulation of IL-8 in human melanoma cells.

Discussion

The preferential sensitivity of melanoma cells to small molecule prooxidant intervention [12–16,18] and the documented anti-melanoma activity of electrophilic agents that share a Michael acceptor pharmacophore including curcumin [40,41], dimethylfumarate [15], tomentosin, and inuviscolide [42] lead us to evaluate the anti-melanoma activity of CA *in vitro* and *in vivo*. CA, a key flavor compound contained in the essential oil of cinnamon, contains an electrophilic Michael acceptor pharmacophore that has previously been implicated in the mechanism of CA-induced upregulation of the Nrf2-regulated antioxidant response in cultured human skin cells [32] and inhibition of NFκB inflammatory signaling in endothelial cells [38].

First, we demonstrated that oral administration of CA impairs growth of A375 human melanoma xenografts in SCID mice. Daily administration of CA (120 mg/kg/d in methylcellulose/PBS) was well tolerated and resulted in a moderate, yet significant suppression of tumor growth with reduced immunohistochemical staining for the proliferation marker PCNA (Fig. 1). To the best of our knowledge, this is the first report documenting anti-cancer activity of CA *in vivo*. Next, the dose response relationship of the anti-proliferative activity of CA against cultured human melanoma and colon cancer cells was established (Fig. 2 and table 1). Inhibition of proliferation of A375 human melanoma cells and suppression of DNA synthesis (Fig. 3) occurred at low micromolar concentrations of CA, but was not observed with Michael-inactive CA-derivatives. Moreover, melanoma cell invasiveness through basement membrane was significantly impaired by CA pre-treatment (Fig. 5). Indicative of rapid induction of an oxidative stress response by CA treatment, intracellular ROS were elevated dose dependently (Fig. 6E), and upregulated expression of established (oxidative) stress response genes including HMOX1, SRXN1, GPX2, TXNRD1, CDKN1A, DDIT3, and EGR1 was detected by array analysis (Fig. 6A-B) [43]. Remarkably, at concentrations of CA (10 and

20 μM) that elevated cellular ROS levels, cellular glutathione levels also were upregulated, suggesting that redox alterations induced by CA treatment are complex and likely result from an overlap of stress-induced and counterbalancing antioxidant response pathways. Future experiments will address the question if activation of the electrophilic stress-sensitive transcription factor Nrf2, shown earlier to mediate upregulation of antioxidant gene expression in human fibroblasts and keratinocytes exposed to CA [32], is involved in the stress response of melanoma cells to CA treatment observed in this study. Interestingly, upregulation of cellular glutathione content and heme oxygenase-1 protein levels in response to exposure to non-cytotoxic concentrations of acrolein and cinnamic aldehyde has already been demonstrated in human endothelial cells and mechanistically linked to Nrf2-activation [26].

Consistent with CA-induction of G1 cell cycle arrest in A375 melanoma cells, the oxidative stress responsive cyclin dependent kinase inhibitor p21 encoded by CDKN1A was strongly upregulated (Fig. 6A, B, and D), a potential molecular mechanism of CA anti-proliferative activity reminiscent of p21-mediated G1 arrest in HT29 colon cancer cells under oxidative stress from sulforaphane treatment [44, 45]. In this context, it will be important to further explore the mechanistic role of other gene expression changes detected in our array analysis, particularly the involvement of CA-induced upregulation of EGR1 and DDIT3 (also called growth arrest and DNA damage inducible gene 153, GADD153). These are important oxidative stress-responsive transcription factors regulated at the transcriptional level that have been shown to mediate growth arrest and apoptosis in various cancer cell lines exposed to oxidative stress [46–49].

NFκB is a redox sensitive oncogenic transcription factor involved in human metastatic melanoma [6,9,39]. Gene mutations reported with high frequency in metastatic melanoma including $p16^{INK4a}$, $p14^{INK4/ARF}$, N-Ras, B-Raf, and PTEN have been shown to be associated with NF-κB upregulation involved in regulation of proliferation, survival, invasion, angiogenesis, and metastasis [39]. NFκB thus represents a promising target for melanoma chemoprevention and chemotherapy. Various small molecule electrophilic Michael acceptors are documented inhibitors of NFκB in melanoma cells [15,41,42]. For example, curcumin-induced antiproliferative and proapoptotic effects in melanoma cells are associated with suppression of IκB kinase and NFκB activity [41]. Moreover, induction of melanoma cell cycle arrest and apoptosis, with inhibition of NFκB and upregulation of p21 have been described for the sesquiterpene lactones tomentosin and Inuviscolide that contain an α-methylene-γ-lactone Michael acceptor pharmacophore capable of forming covalent Michael adducts with the nucleophilic sites of biological molecules [42]. Recently, inhibition of NFkB by the cinnamon ingredients CA and MCA has been demonstrated in human macrophages [50], and CA-suppression of NFκB inflammatory signaling in endothelial cells has been shown to occur as a result of inhibition of IκB-α degradation and HO-1 activation with suppression of TNFα-induced p65 translocation [38]. Moreover, in another study examining renal tissue of aged rats, dietary administration of CA inhibited NF-κB activation through the ERK and p38 MAPK pathways [30]. We therefore tested the hypothesis that the electrophilic Michael acceptor CA may target NFκB transcriptional activity and NFκB-mediated inflammatory signaling in human melanoma cells. Our experiments using a luciferase reporter construct demonstrated that CA inhibits NFκB constitutive and TNFα-induced transcriptional activity, an activity absent from non-Michael reactive CA-derivatives including DHCA, CAC, and COH (Fig. 7). Future experiments must therefore address the exact molecular mechanism of CA-induced suppression of NFκB transcriptional activity in A375 melanoma cells as observed in our studies.

It is now well established that melanoma tumor progression occurs through autocrine signaling pathways that include NF-κB-regulated chemokines including IL-8 (also known as CXCL-8) [39]. Overexpression of IL-8 causes metastatic tumor progression in primary melanoma cells

[51,52] and is associated with the transition from radial to vertical growth phase in melanoma [53]. Indeed, pronounced inhibition of TNFα-induced IL-8 expression by CA occurred in the low micromolar range in human A375 melanoma cells as shown in Fig. 8, representing a potentially important mechanism of CA anti-melanoma activity.

In summary, our findings demonstrate for the first time that oral administration of CA exerts significant anti-melanoma activity in an animal model of the disease and suggest that CA anti-proliferative and anti-NFκB activity observed in melanoma cell culture depend on Michael acceptor reactivity associated with this dietary electrophile. Additional studies must address the detailed molecular mechanism of CA anti-melanoma activity and will employ proteomic tools for the identification of CA-adducted cellular targets, such as protein thiol residues in redox sensitive factors including molecular components of the Nrf2 and NFκB signaling cascades. It is important to note that anti-melanoma activity *in vivo* was observed at high oral doses of CA, not achievable through dietary intake of CA-containing foods where typical concentrations do not exceed the lower mg/kg range [23]. However, based on the significant anti-melanoma activity of CA that we observed at well-tolerated high oral doses, future studies should further examine the mostly unexplored chemopreventive and chemotherapeutic potential of this dietary Michael acceptor.

Acknowledgements

Supported in part by grants from the National Institutes of Health [R01CA122484, ES007091, Arizona Cancer Center Support Grant CA023074], and from the Arizona Biomedical Research Commission (ABRC 0721). Animal experimentation was performed at the AZCC experimental mouse shared service (EMSS), and tumor histology was performed at the tissue acquisition and cellular/molecular analysis shared service (TACMASS).

Abbreviations

7-AAD
7-Amino-actinomycin D

AV
annexinV

BrdU
5-bromo-2′-deoxyuridine

CA
trans-cinnamic aldehyde

CAC
cinnamic acid

CDKN1A
cyclin-dependent kinase inhibitor 1A

COH
cinnamic alcohol

DCFH-DA
2′,7′-dichlorodihydrofluorescein diacetate

DHCA
dihydrocinnamic aldehyde

DDIT3
DNA-damage-inducible transcript 3

EGR1
early growth response gene 1

FITC
fluorescein isothiocyanate

GPX2
glutathione peroxidase 2

HMOX1
heme oxygenase-1

MCA
2-methoxy-trans-cinnamic aldehyde

NFκB
nuclear factor kappa B

PI
propidium iodide

PCNA
proliferating cell nuclear antigen

q.d
quaque die/every day

ROS
reactive oxygen species

SDS-PAGE
sodium dodecylsulfate polyacrylamide gel electrophoresis

SRXN1
sulfiredoxin 1 homolog

TXNRD1
thioredoxin reductase 1

References

1. Lens MB, Dawes M. Global perspectives of contemporary epidemiological trends of cutaneous malignant melanoma. Br J Dermatol 2004;150:179–85. [PubMed: 14996086]
2. Qin JZ, Stennett L, Bacon P, Bodner B, Hendrix MJ, Seftor RE, et al. p53-independent NOXA induction overcomes apoptotic resistance of malignant melanomas. Mol Cancer Ther 2004;3:895–902. [PubMed: 15299072]
3. Wondrak GT, Jacobson MK, Jacobson EL. An Emerging Molecular Target in Melanoma: Cellular Carbonyl Stress and the Inhibition of Mitochondrial Survival Pathways by Carbonyl Scavenger Agents. Curr Cancer Ther Rev 2005;1:271–6.
4. Meyskens FL Jr, Farmer PJ, Yang S, Anton-Culver H. New perspectives on melanoma pathogenesis and chemoprevention. Recent Results Cancer Res 2007;174:191–5. [PubMed: 17302196]
5. Eberle J, Kurbanov BM, Hossini AM, Trefzer U, Fecker LF. Overcoming apoptosis deficiency of melanoma-hope for new therapeutic approaches. Drug Resist Updat 2007;10:218–34. [PubMed: 18054518]
6. Brar SS, Kennedy TP, Whorton AR, Sturrock AB, Hueckstead TP, Ghio AJ, et al. Reactive oxygen species from NAD(P)H:quinone oxidoreductase constitutively activate NF-kappaB in malignant melanoma cells. Am J Physiol Cell Physiol 2001;280:C659–76. [PubMed: 11171586]

7. Govindarajan B, Sligh JE, Vincent BJ, Li M, Canter JA, Nickoloff BJ, et al. Overexpression of Akt converts radial growth melanoma to vertical growth melanoma. J Clin Invest 2007;117:719–29. [PubMed: 17318262]
8. Fruehauf JP, Meyskens FL Jr. Reactive oxygen species: a breath of life or death? Clin Cancer Res 2007;13:789–94. [PubMed: 17289868]
9. Fried L, Arbiser JL. The reactive oxygen-driven tumor: relevance to melanoma. Pigment Cell Melanoma Res 2008;21:117–22. [PubMed: 18384505]
10. Brar SS, Kennedy TP, Sturrock AB, Huecksteadt TP, Quinn MT, Whorton AR, et al. An NAD(P)H oxidase regulates growth and transcription in melanoma cells. Am J Physiol Cell Physiol 2002;282:C1212–24. [PubMed: 11997235]
11. Engel RH, Evens AM. Oxidative stress and apoptosis: a new treatment paradigm in cancer. Front Biosci 2006;11:300–12. [PubMed: 16146732]
12. Cabello CM, Bair WB 3rd, Wondrak GT. Experimental therapeutics: targeting the redox Achilles heel of cancer. Curr Opin Investig Drugs 2007;8:1022–37.
13. Cen D, Brayton D, Shahandeh B, Meyskens FL Jr, Farmer PJ. Disulfiram facilitates intracellular Cu uptake and induces apoptosis in human melanoma cells. J Med Chem 2004;47:6914–20. [PubMed: 15615540]
14. Wondrak GT. NQO1-activated phenothiazinium redox cyclers for the targeted bioreductive induction of cancer cell apoptosis. Free Radic Biol Med 2007;43:178–90. [PubMed: 17603928]
15. Loewe R, Valero T, Kremling S, Pratscher B, Kunstfeld R, Pehamberger H, et al. Dimethylfumarate impairs melanoma growth and metastasis. Cancer Res 2006;66:11888–96. [PubMed: 17178886]
16. Wang CC, Chiang YM, Sung SC, Hsu YL, Chang JK, Kuo PL. Plumbagin induces cell cycle arrest and apoptosis through reactive oxygen species/c-Jun N-terminal kinase pathways in human melanoma A375. S2 cells Cancer Lett 2008;259:82–98.
17. Magda D, Miller RA. Motexafin gadolinium: a novel redox active drug for cancer therapy. Semin Cancer Biol 2006;16:466–76. [PubMed: 17112739]
18. Tuma RS. Reactive oxygen species may have antitumor activity in metastatic melanoma. J Natl Cancer Inst 2008;100:11–2. [PubMed: 18159075]
19. Esterbauer H, Schaur RJ, Zollner H. Chemistry and biochemistry of 4-hydroxynonenal, malonaldehyde and related aldehydes. Free Radic Biol Med 1991;11:81–128. [PubMed: 1937131]
20. Kurtz AJ, Lloyd RS. 1, N2-deoxyguanosine adducts of acrolein, crotonaldehyde, and trans-4-hydroxynonenal cross-link to peptides via Schiff base linkage. J Biol Chem 2003;278:5970–6. [PubMed: 12502710]
21. O'Brien PJ, Siraki AG, Shangari N. Aldehyde sources, metabolism, molecular toxicity mechanisms, and possible effects on human health. Crit Rev Toxicol 2005;35:609–62. [PubMed: 16417045]
22. Chan K, Poon R, O'Brien PJ. Application of structure-activity relationships to investigate the molecular mechanisms of hepatocyte toxicity and electrophilic reactivity of alpha, beta-unsaturated aldehydes. J Appl Toxicol. 2008
23. Friedman M, Kozukue N, Harden LA. Cinnamaldehyde content in foods determined by gas chromatography-mass spectrometry. J Agric Food Chem 2000;48:5702–9. [PubMed: 11087542]
24. Peters MM, Caldwell J. Studies on trans-cinnamaldehyde. 1 The influence of dose size and sex on its disposition in the rat and mouse. Food Chem Toxicol 1994;32:869–76. [PubMed: 7959441]
25. NTP (National Toxicology Program) Technical Report on the Toxicology and Carcinogenesis Studies of trans-Cinnamaldehyde. NTP TR 514, NIH Publication No 04–4448, 2004.
26. Wu CC, Hsieh CW, Lai PH, Lin JB, Liu YC, Wung BS. Upregulation of endothelial heme oxygenase-1 expression through the activation of the JNK pathway by sublethal concentrations of acrolein. Toxicol Appl Pharmacol 2006;214:244–52. [PubMed: 16480751]
27. Singh G, Maurya S, DeLampasona MP, Catalan CA. A comparison of chemical, antioxidant and antimicrobial studies of cinnamon leaf and bark volatile oils, oleoresins and their constituents. Food Chem Toxicol 2007;45:1650–61. [PubMed: 17408833]
28. Matan N, Rimkeeree H, Mawson AJ, Chompreeda P, Haruthaithanasan V, Parker M. Antimicrobial activity of cinnamon and clove oils under modified atmosphere conditions. Int J Food Microbiol 2006;107:180–5. [PubMed: 16266767]

29. Kurokawa M, Kumeda CA, Yamamura J, Kamiyama T, Shiraki K. Antipyretic activity of cinnamyl derivatives and related compounds in influenza virus-infected mice. Eur J Pharmacol 1998;348:45–51. [PubMed: 9650830]
30. Kim DH, Kim CH, Kim MS, Kim JY, Jung KJ, Chung JH, et al. Suppression of age-related inflammatory NF-kappaB activation by cinnamaldehyde. Biogerontology 2007;8:545–54. [PubMed: 17486422]
31. Anderson RA, Broadhurst CL, Polansky MM, Schmidt WF, Khan A, Flanagan VP, et al. Isolation and characterization of polyphenol type-A polymers from cinnamon with insulin-like biological activity. J Agric Food Chem 2004;52:65–70. [PubMed: 14709014]
32. Wondrak GT, Cabello CM, Villeneuve NF, Zhang S, Ley S, Li Y, et al. Cinnamoyl-based Nrf2-activators targeting human skin cell photo-oxidative stress. Free Radic Biol Med 2008;45:385–95. [PubMed: 18482591]
33. Wondrak GT, Jacobson MK, Jacobson EL. Antimelanoma activity of apoptogenic carbonyl scavengers. J Pharmacol Exp Ther 2006;316:805–14. [PubMed: 16210394]
34. Wondrak GT, Roberts MJ, Jacobson MK, Jacobson EL. 3-hydroxypyridine chromophores are endogenous sensitizers of photooxidative stress in human skin cells. J Biol Chem 2004;279:30009–20. [PubMed: 15133022]
35. Pani G, Colavitti R, Bedogni B, Anzevino R, Borrello S, Galeotti T. Determination of intracellular reactive oxygen species as function of cell density. Methods Enzymol 2002;352:91–100. [PubMed: 12125380]
36. Jenner PM, Hagan EC, Taylor JM, Cook EL, Fitzhugh OG. Food flavourings and compounds of related structure. I. Acute oral toxicity. Food Cosmet Toxicol 1964;2:327–43.
37. Cortese MM, Suschek CV, Wetzel W, Kroncke KD, Kolb-Bachofen V. Zinc protects endothelial cells from hydrogen peroxide via Nrf2-dependent stimulation of glutathione biosynthesis. Free Radic Biol Med 2008;44:2002–12. [PubMed: 18355458]
38. Liao BC, Hsieh CW, Liu YC, Tzeng TT, Sun YW, Wung BS. Cinnamaldehyde inhibits the tumor necrosis factor-alpha-induced expression of cell adhesion molecules in endothelial cells by suppressing NF-kappaB activation: Effects upon IkappaB and Nrf2. Toxicol Appl Pharmacol 2008;229:161–71. [PubMed: 18304597]
39. Ueda Y, Richmond A. NF-kappaB activation in melanoma. Pigment Cell Res 2006;19:112–24. [PubMed: 16524427]
40. Iersel ML, Ploemen JP, Struik I, van Amersfoort C, Keyzer AE, Schefferlie JG, et al. Inhibition of glutathione S-transferase activity in human melanoma cells by alpha, beta-unsaturated carbonyl derivatives. Effects of acrolein, cinnamaldehyde, citral, crotonaldehyde, curcumin, ethacrynic acid, and trans-2-hexenal. Chem Biol Interact 1996;102:117–32. [PubMed: 8950226]
41. Siwak DR, Shishodia S, Aggarwal BB, Kurzrock R. Curcumin-induced antiproliferative and proapoptotic effects in melanoma cells are associated with suppression of IkappaB kinase and nuclear factor kappaB activity and are independent of the B-Raf/mitogen-activated/extracellular signal-regulated protein kinase pathway and the Akt pathway. Cancer 2005;104:879–90. [PubMed: 16007726]
42. Rozenblat S, Grossman S, Bergman M, Gottlieb H, Cohen Y, Dovrat S. Induction of G2/M arrest and apoptosis by sesquiterpene lactones in human melanoma cell lines. Biochem Pharmacol 2008;75:369–82. [PubMed: 17919456]
43. Han ES, Muller FL, Perez V, Qi W, Liang H, Xi L, et al. The in vivo Gene Expression Signature of Oxidative Stress. Physiol Genomics. 2008
44. O'Reilly MA. Redox activation of p21Cip1/WAF1/Sdi1: a multifunctional regulator of cell survival and death. Antioxid Redox Signal 2005;7:108–18. [PubMed: 15650400]
45. Shen G, Xu C, Chen C, Hebbar V, Kong AN. p53-independent G1 cell cycle arrest of human colon carcinoma cells HT-29 by sulforaphane is associated with induction of p21CIP1 and inhibition of expression of cyclin D1. Cancer Chemother Pharmacol 2006;57:317–27. [PubMed: 16170570]
46. Maytin EV, Ubeda M, Lin JC, Habener JF. Stress-inducible transcription factor CHOP/gadd153 induces apoptosis in mammalian cells via p38 kinase-dependent and -independent mechanisms. Exp Cell Res 2001;267:193–204. [PubMed: 11426938]

47. Wen J, You KR, Lee SY, Song CH, Kim DG. Oxidative stress-mediated apoptosis. The anticancer effect of the sesquiterpene lactone parthenolide. J Biol Chem 2002;277:38954–64. [PubMed: 12151389]

48. Stuart JR, Kawai H, Tsai KK, Chuang EY, Yuan ZM. c-Abl regulates early growth response protein (EGR1) in response to oxidative stress. Oncogene 2005;24:8085–92. [PubMed: 16091742]

49. Gibbs JD, Liebermann DA, Hoffman B. Egr-1 abrogates the E2F-1 block in terminal myeloid differentiation and suppresses leukemia. Oncogene 2008;27:98–106. [PubMed: 17599039]

50. Reddy AM, Seo JH, Ryu SY, Kim YS, Kim YS, Min KR, et al. Cinnamaldehyde and 2-methoxycinnamaldehyde as NF-kappaB inhibitors from Cinnamomum cassia. Planta Med 2004;70:823–7. [PubMed: 15503352]

51. Singh RK, Varney ML, Bucana CD, Johansson SL. Expression of interleukin-8 in primary and metastatic malignant melanoma of the skin. Melanoma Res 1999;9:383–7. [PubMed: 10504057]

52. Schaider H, Oka M, Bogenrieder T, Nesbit M, Satyamoorthy K, Berking C, et al. Differential response of primary and metastatic melanomas to neutrophils attracted by IL-8. Int J Cancer 2003;103:335–43. [PubMed: 12471616]

53. Leslie MC, Bar-Eli M. Regulation of gene expression in melanoma: new approaches for treatment. J Cell Biochem 2005;94:25–38. [PubMed: 15523674]

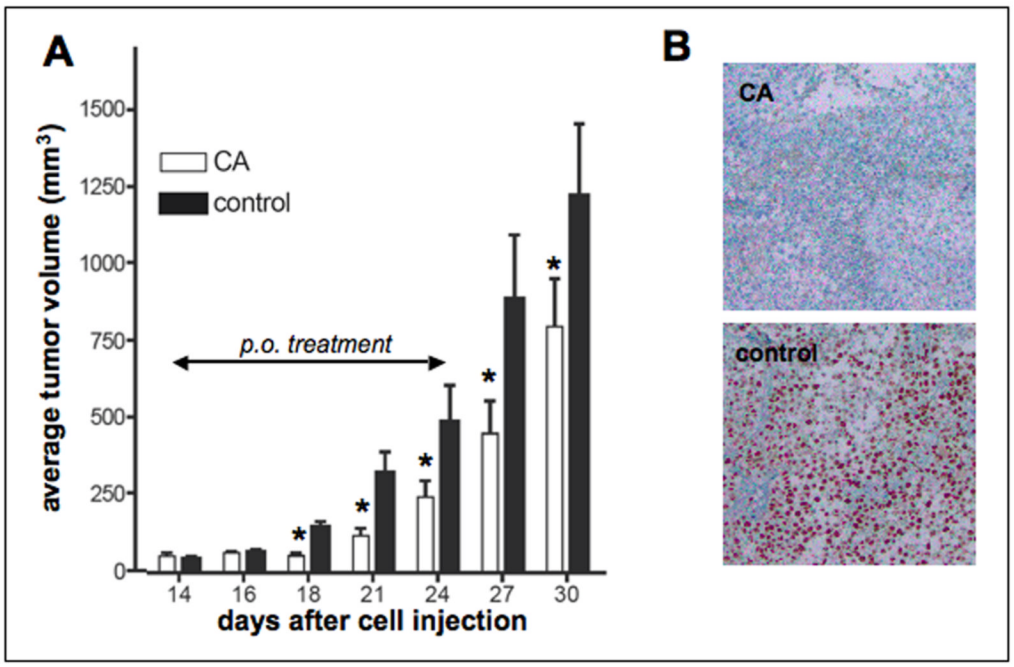

Figure 1. Cinnamic aldehyde inhibits tumor growth in a human melanoma SCID-mouse xenograft model

Human A375 melanoma cells (10×10^6) were implanted s.c. into the right flank of SCID mice. 14 days after cell injection animals were pair-matched (65 mm^3 average tumor size) and daily treatment (CA, 120 mg/kg/d in methylcellulose/PBS, n=10) was initiated by oral gavage. Control animals (n=12) received carrier only. (A) Tumor growth curves were obtained by determining average tumor volumes until day 30 after cell injection. Data points are depicted as means ± SEM and statistical comparison between individual data point was performed using the two-sided Student's *t* test (*, $p < 0.05$; **, $p < 0.01$; ***, $p < 0.001$). (B) Immunohistochemical staining for PCNA using primary tumor tissue of CA-treated and carrier-treated mice sacrificed on day 34 (n = 2, each group). Paraformaldehyde-fixed, paraffin-embedded 5 μm sections were analyzed using a mouse monoclonal antibody to PCNA followed by biotinylated-streptavidin-HRP/DAB visualization. Hematoxylin counterstaining was also performed. Photographs representative of five high power fields taken per tissue section are shown.

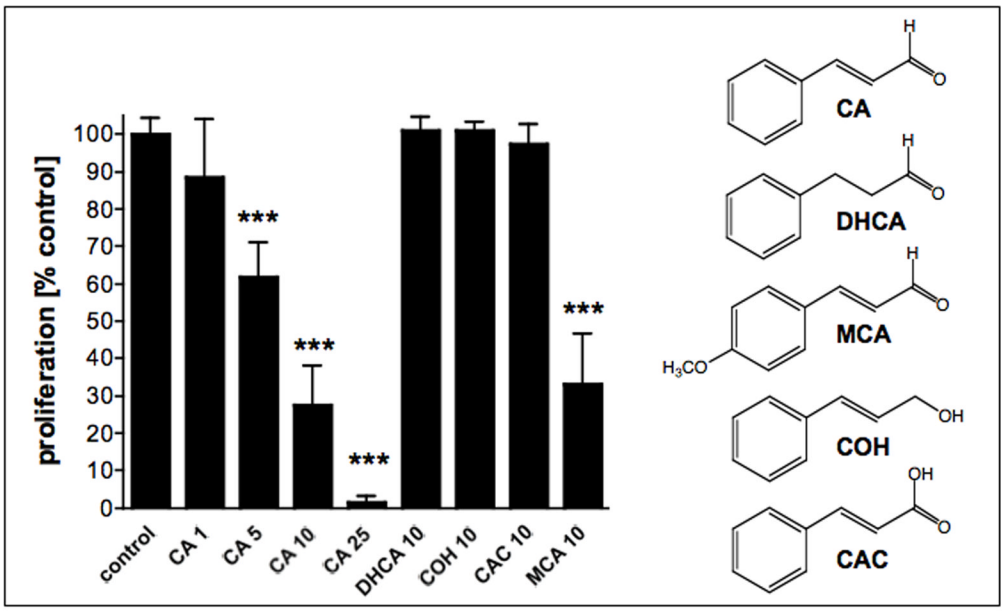

Figure 2. Cinnamic aldehyde, but not its Michael-inactive derivatives, inhibits proliferation of human A375 melanoma cells

Anti-proliferative activity of CA and CA-derivatives (DHCA, COH, CAC, and MCA; molecular structures as indicated) was assessed using human A375 melanoma cells (mean ± SD, n=3) as described in Materials and Methods. Numbers indicate concentration of test compound in μM. Proliferation was compared with control cells that received mock treatment.

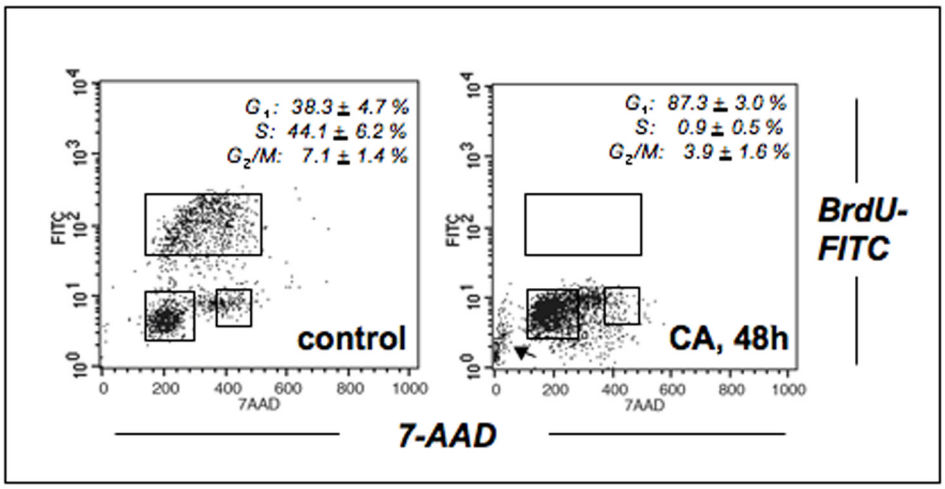

Figure 3. Cinnamic aldehyde suppresses DNA synthesis and induces G1-phase cell cycle arrest in human A375 melanoma cells

Human A375 melanoma cells were exposed to CA (20 μM, 48 h), and bivariate cell cycle analysis was performed by flow cytometric determination of cellular DNA synthesis (BrdU incorporation) and DNA content (7-AAD staining). The numbers indicate cells in G1, S, and G2/M phase, respectively, in percent of total gated cells (mean ± SD, n=3). The arrow marks a small fraction (approx. 8%) of apoptotic cells in sub-G1.

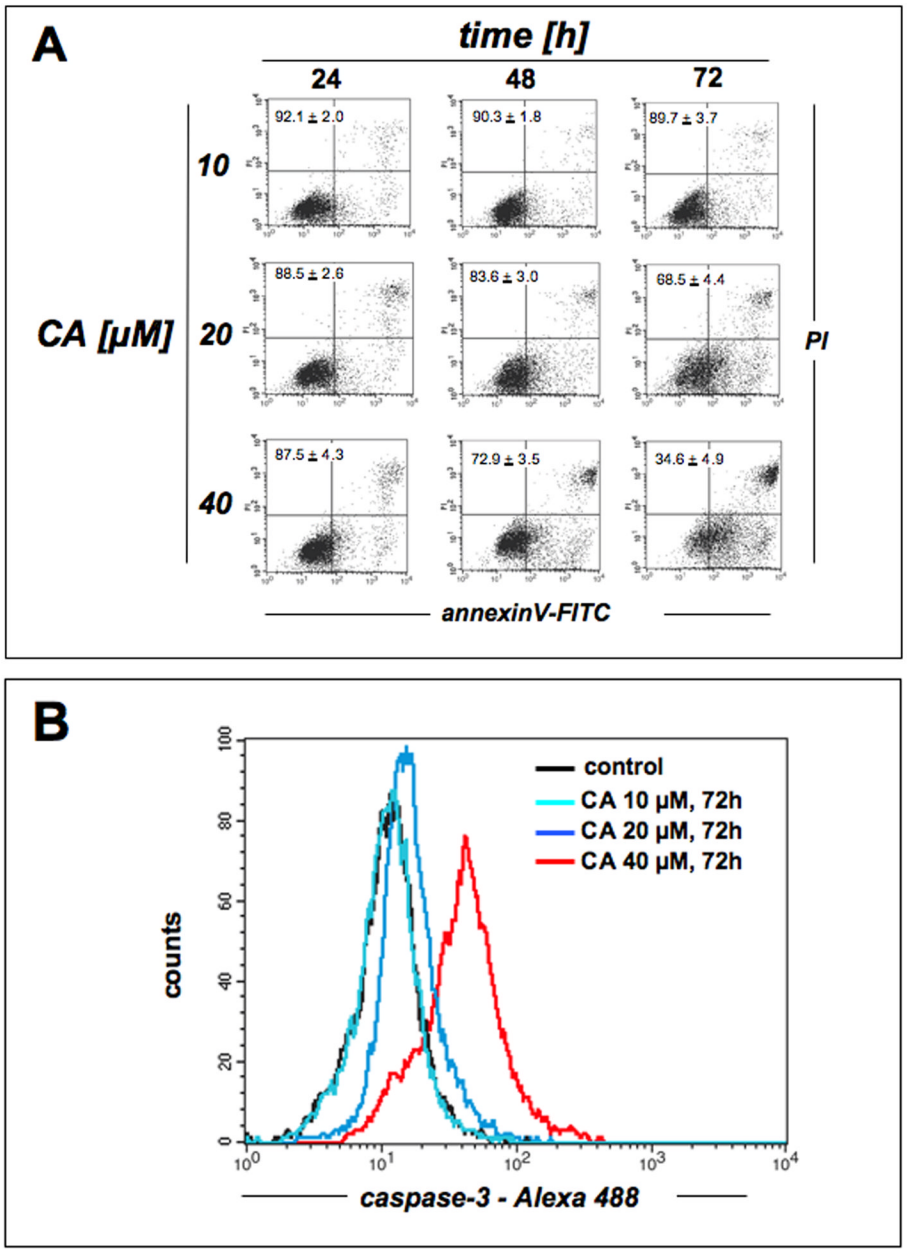

Figure 4. Prolonged exposure to cinnamic aldehyde dose-dependently induces apoptosis with procaspase-3 cleavage in human A375 melanoma cells

(A) Time course (24, 48, and 72 h) of induction of cell death by exposure to increasing doses of CA (10, 20, and 40 μM) was assessed by flow cytometric analysis of annexinV-FITC/ propidium iodide-stained cells. The numbers indicate viable cells (AV^-, PI^-, lower left quadrant) in percent of total gated cells (mean ± SD, n=3). (Viability of untreated controls was 92.1 ± 1.0 %; data not shown). (B) CA-induced (10, 20, and 40 μM, 72 h) caspase-3 activation was examined by flow cytometric detection using an Alexa Fluor 488-conjugated monoclonal antibody against cleaved procaspase-3. One representative experiment of three similar repeats is shown.

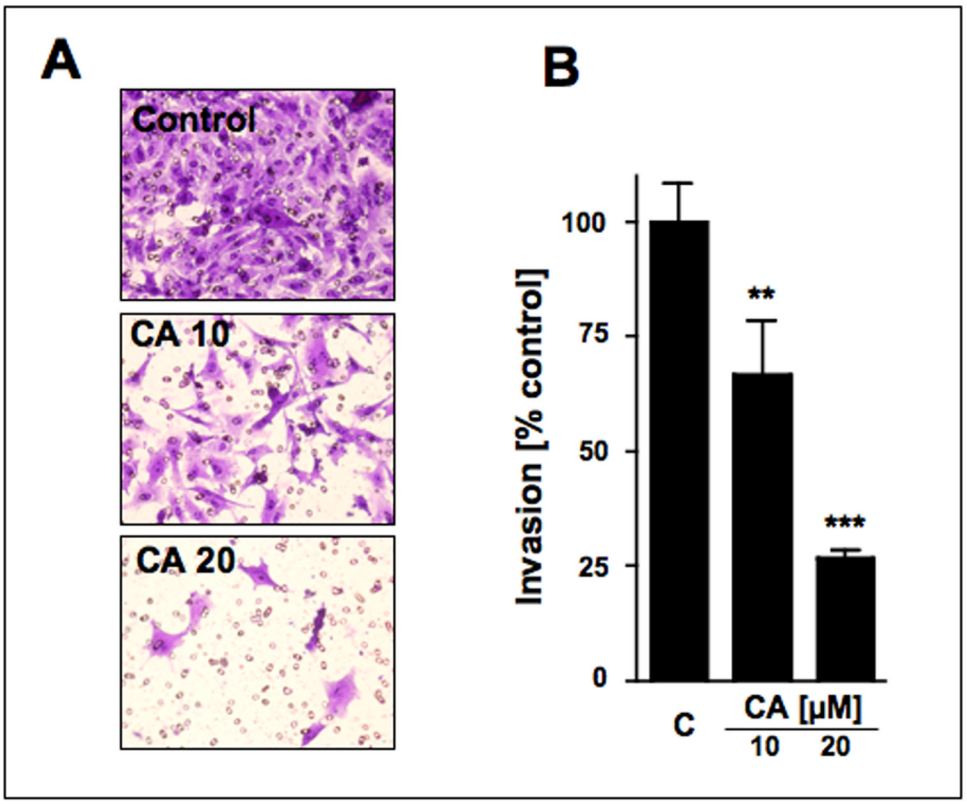

Figure 5. Cinnamic aldehyde impairs invasiveness of human A375 melanoma cells

Melanoma cell invasion through basement membrane extracellular matrix was determined using the CytoSelect™ Cell Invasion Assay as detailed in Materials and Methods. Invasion of A375 cells (over a 48 h period) left untreated or treated with CA (10 or 20 μM) was assessed by crystal violet staining of cells that passed through the basement membrane clinging to the bottom of the Boyden chamber membrane. (A) CA-Modulation of melanoma cell invasiveness assessed by light microscopy. A representative result of three similar repeats is shown. (B) Colorimetric analysis (absorbance at 560 nm) of CA-modulation of melanoma cell invasiveness (mean ± SD, n=3).

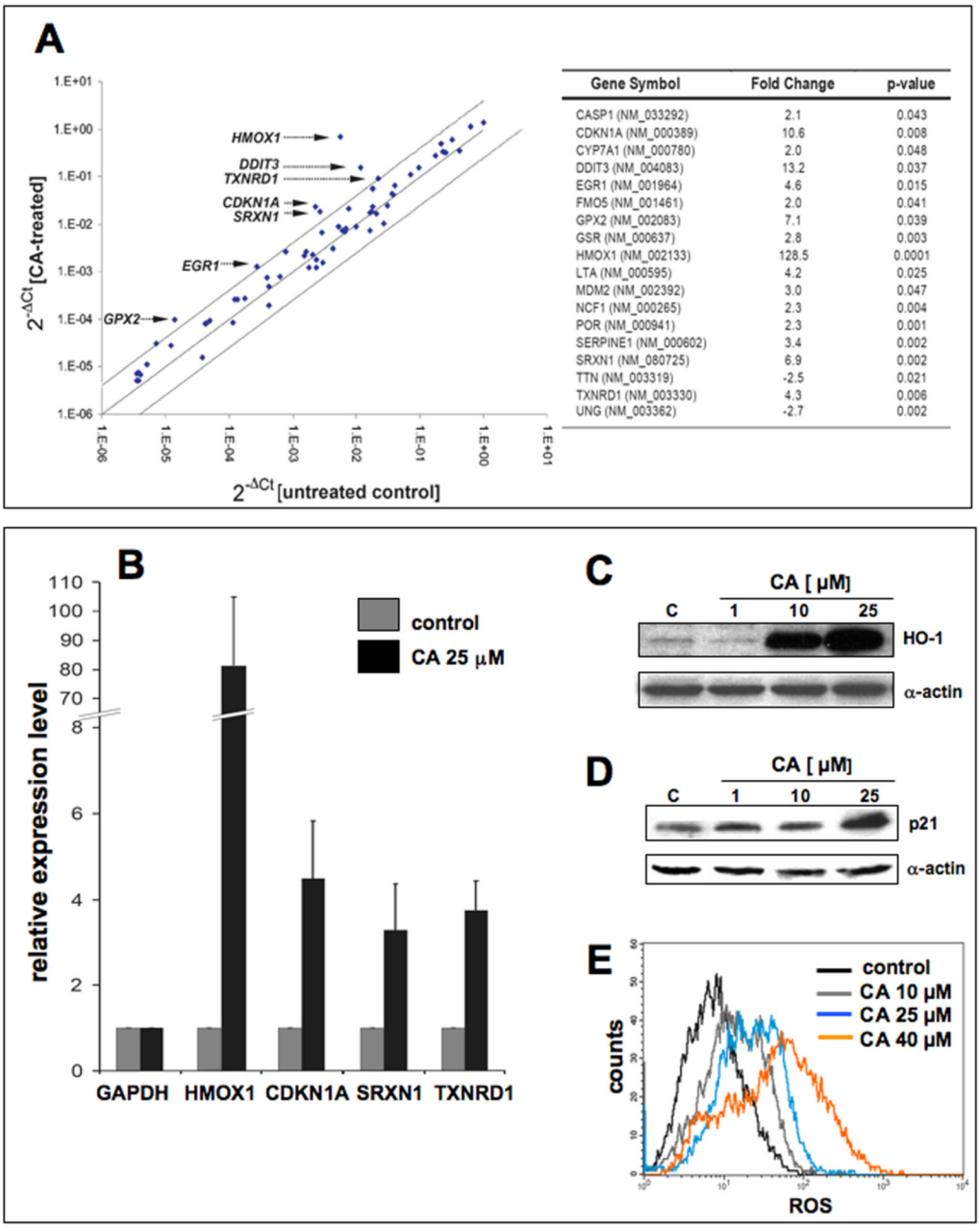

Gene Symbol	Fold Change	p-value
CASP1 (NM_033292)	2.1	0.043
CDKN1A (NM_000389)	10.6	0.008
CYP7A1 (NM_000780)	2.0	0.048
DDIT3 (NM_004083)	13.2	0.037
EGR1 (NM_001964)	4.6	0.015
FMO5 (NM_001461)	2.0	0.041
GPX2 (NM_002083)	7.1	0.039
GSR (NM_000637)	2.8	0.003
HMOX1 (NM_002133)	128.5	0.0001
LTA (NM_000595)	4.2	0.025
MDM2 (NM_002392)	3.0	0.047
NCF1 (NM_000265)	2.3	0.004
POR (NM_000941)	2.3	0.001
SERPINE1 (NM_000602)	3.4	0.002
SRXN1 (NM_080725)	6.9	0.002
TTN (NM_003319)	-2.5	0.021
TXNRD1 (NM_003330)	4.3	0.006
UNG (NM_003362)	-2.7	0.002

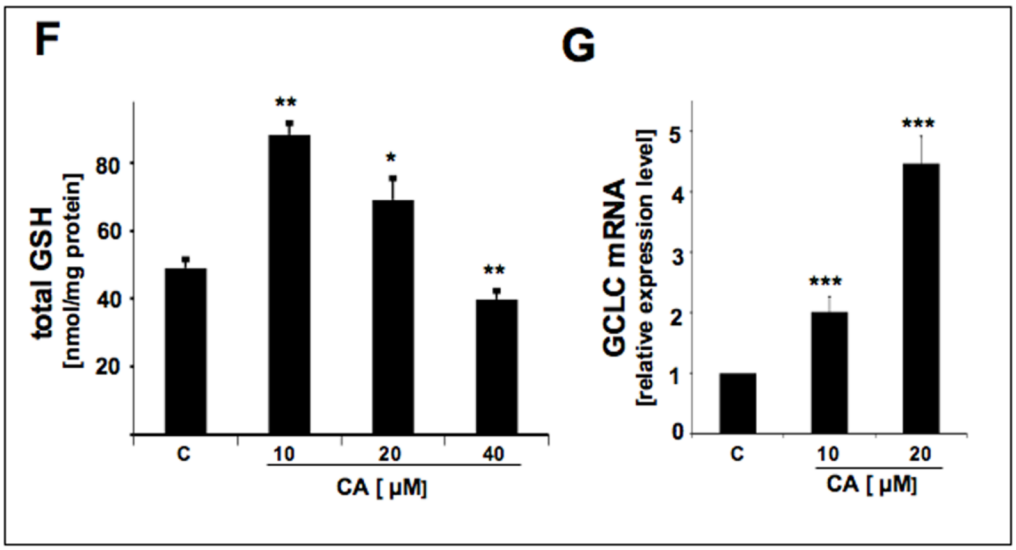

Figure 6. Cinnamic aldehyde induces oxidative stress and oxidative stress response gene expression in human A375 melanoma cells

(A) CA-induced gene expression changes in A375 human melanoma cells. The scatter blot (left panel) depicts differential gene expression as detected by the RT^2 Human Oxidative Stress Profiler™ PCR Expression Array technology profiling the expression of 84 oxidative stress-related genes after CA treatment (25 μM, 24 h; three independent experiments). Upper and lower lines represent the cut-off indicating four fold up- or down-regulated expression, respectively. Arrows specify genes with at least 4 fold up-regulated expression versus untreated controls. The table (right panel) summarizes all genes that are at least two-fold upregulated in response to CA treatment. (B) Human A375 melanoma cells were cultured for 24h in the presence of CA (25 μM) or left untreated. Total RNA was prepared and gene expression of HMOX1, CDKN1A, SRXN1, TXNRD1 was then quantitatively examined using real time RT-PCR analysis with normalization for GAPDH expression levels. Relative expression levels in response to mock treatment (control) and exposure to CA were determined in three repeat experiments (n=3, mean ± SD). (C) CA-modulation of cellular heme oxygenase-1 (HO-1) protein levels and (D) CA-modulation of cellular p21 protein levels were examined in total cellular protein extracts by 15% SDS-PAGE followed by immunoblot detection using enhanced chemiluminescence. Detection of α-actin expression served as a loading control. (E) Induction of intracellular oxidative stress in human A375 melanoma cells by treatment with CA. Cells were exposed to CA (10 and 25 μM, 24 h) and intracellular oxidative stress was assessed by 2′,7′-dichloro-dihydrofluorescein diacetate staining followed by flow cytometric analysis. One representative experiment of three similar repeats is shown. (F) Modulation of intracellular glutathione content in A375 melanoma cells exposed to increasing concentrations of CA (10–40 μM, 24 h). Total glutathione content was normalized to protein content. (G) Upregulation of GCLC gene expression assessed by real time RT-PCR analysis with normalization for β-actin expression levels in A375 melanoma cells exposed to increasing concentrations of CA (10–20 μM, 24 h).

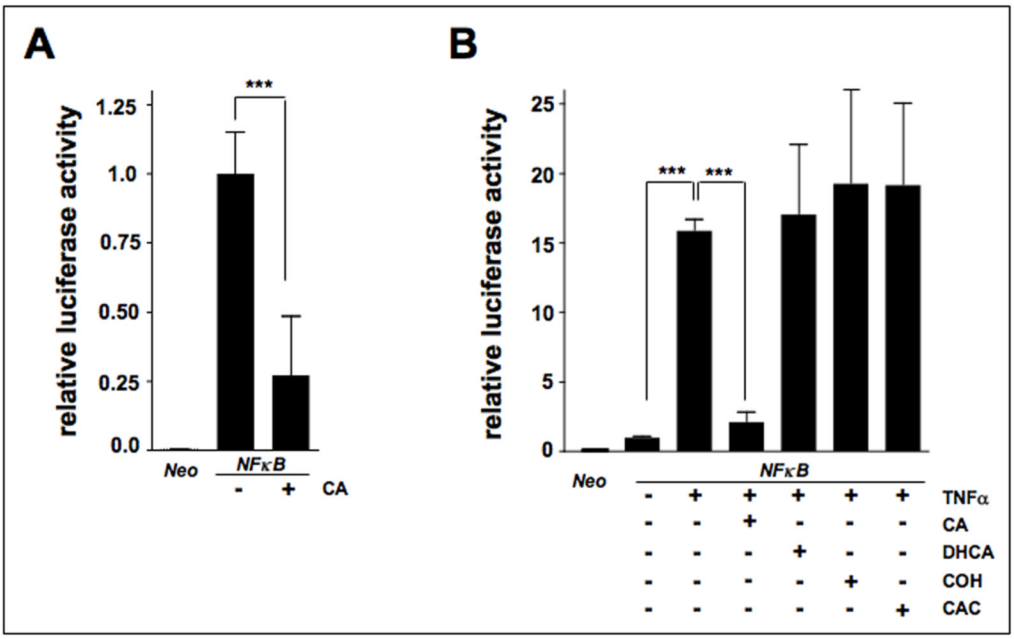

Figure 7. Cinnamic aldehyde inhibits constitutive and TNFα-induced NFκB transcriptional activity in human melanoma cells

A375 melanoma cells were cotransfected with a plasmid containing a firefly luciferase reporter gene under the control of the NFκB promotor and a plasmid encoding renilla luciferase for normalization of transfection efficiency. (A) Suppression of constitutive NFkB transcriptional activity was examined in cells treated with CA (20 μM) for 12 h. (B) Suppression of TNFα-induced NFkB transcriptional activity was examined in cells that were pretreated with CA, DHCA, COH, and CAC (20 μM each, 3h exposure) followed by TNFα treatment (20ng/mL, 12h exposure) and determination of luciferase activity. Potency of fold-induction is expressed as luciferase activity in relative luminescence units versus untreated control transfectants (mean ± SD, n≥3).

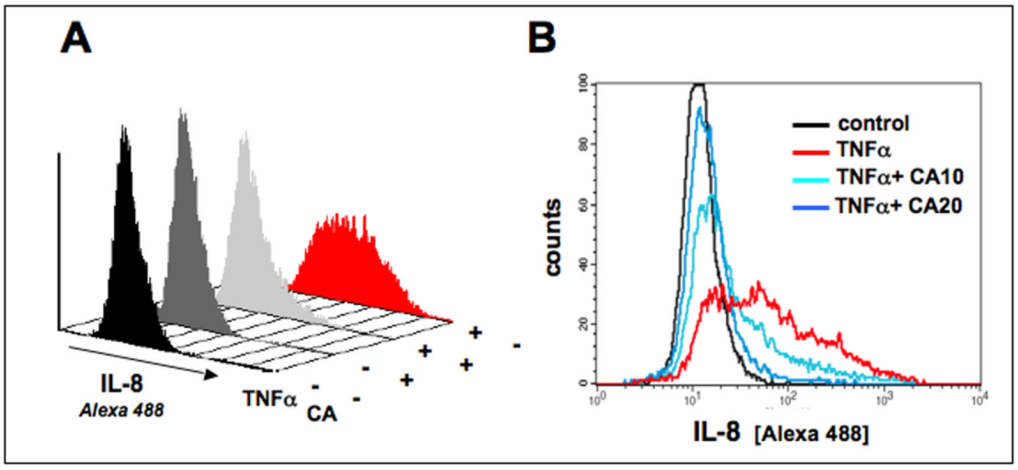

Figure 8. Cinnamic aldehyde inhibits TNFα-induced expression of IL-8 in A375 melanoma cells

A375 cells were pretreated with CA for 3 h and then exposed to TNFα. After 6 h, IL-8 expression was examined in CA- and mock-pretreated cells by flow cytometric analysis using an Alexa 488-conjugated mouse monoclonal antibody directed against human IL-8. (A) Modulation of IL-8 expression by CA (20 μM) pretreatment followed by TNFα stimulation. (B) Dose response relationship of inhibition of TNFα-induced IL-8 expression by CA (10 and 20 μM) pretreatment. One representative experiment out of at least three similar repeats is shown.

Table 1

Cinnamic aldehyde antiproliferative activity against human melanoma and colon cancer cell lines

IC_{50} values of CA-induced inhibition of proliferation of human melanoma (A375, G361, LOX), colon cancer (HT29, HCT116) cell lines (mean ± SD, n=3), and normal primary skin cells (Hs27 fibroblasts, HEK keratinocytes) were determined in proliferation assays as specified in Materials and Methods.

cell line	IC_{50} [CA, μM]
G361	8.1 ± 2.5
LOX	3.4 ± 0.9
A375	6.3 ± 1.1
HT29	19.7 ± 3.2
HCT116	12.6 ± 3.7
Hs27	21.4 ± 2.2
HEK	17.9 ± 1.6